Int J Clin Exp Pathol 2019;12(4):1204-1213
www.ijcep.com /ISSN:1936-2625/IJCEP0088262

Original Article

Triptolide reduces proliferation and enhances apoptosis in drug-resistant human oral cancer cells

Li Tian[1,4*], Yang Zhang[2*], Yu Wang[3], Ruijie Dang[4], Zhiguang Fu[4], Bin Gu[4], Ning Wen[4]

Departments of [1]Anesthesiology and Perioperative Medicine, [2]Orthopedics, [3]Oncology, State Key Discipline of Cell Biology, Xijing Hospital, The Fourth Military Medical University, Xi'an 710018, Shaanxi, China; [4]Institute of Stomatology, Chinese PLA General Hospital, Beijing 100039, China. [*]Equal contributors.

Received November 12, 2018; Accepted December 27, 2018; Epub April 1, 2019; Published April 15, 2019

Abstract: Triptolide (TPL) is a traditional Chinese medicine that possesses anti-multidrug resistance (MDR) properties against various cancers, including oral cancer. However, the functional roles of TPL in oral cancer cells and its potential ability to overcome MDR have not fully evaluated. Therefore, in this study we used oral cancer cell line SAS to establish Taxol-resistant cell line SAS/Taxol and investigated the effects of TPL on MDR, proliferation, and apoptosis of SAS/Taxol cells. We first demonstrated that TPL overcame MDR in SAS/Taxol cells. In addition, TPL induced prominent proliferation inhibition, cell cycle arrest, and apoptosis of SAS/Taxol cells. Furthermore, the pro-apoptotic effect of TPL on SAS/Taxol cells was dependent on intrinsic and extrinsic apoptotic pathways involved in the activation of caspases. Consistently, TPL successfully hampered oral tumor growth by inducing cell apoptosis in a xenograft mouse model. Overall, these results indicated that TPL circumvented MDR of SAS/Taxol cells by inhibition of proliferation and induction of apoptosis which was partly mediated by the intrinsic and extrinsic apoptotic pathways, suggesting the potential therapeutic value of TPL on Taxol-resistant human oral cancer.

Keywords: Triptolide, oral cancer, multidrug-resistance, proliferation, apoptosis

Introduction

Oral squamous cell carcinoma (OSCC) is the sixth most prevalent malignancy with over 500,000 new cases diagnosed annually worldwide [1]. More than 50% of patients with OSCC die within 5 years [2]. Despite great advances in the understanding of cancer biology and the development of novel chemotherapeutic agents, the prognosis of OSCC patients has remained poor [3]. Thus, it is paramount to discover potential therapeutic drugs for OSCC.

Resistance to current anticancer therapeutics and their side effects are the major obstacles to successful cancer therapy. Among the categories of resistance in cancer therapy, multidrug resistance (MDR) is the main cause of OSCC therapy failure [4, 5]. Reportedly, multidrug resistance protein 1 (MDR1), also known as P-glycoprotein, and multidrug resistance protein 1 (MRP1) are closely associated with MDR of cancers [6]. Accumulating evidence demonstrated that apoptosis resistance is a crucial factor for the carcinogenesis of OSCC and is associated with MDR [7]. Thus, exploring novel agents to target MDR1 and MRP1 by inducing apoptosis is an effective strategy for attenuation of MDR in OSCC.

Triptolide (TPL, the structure shown in **Figure 1A**) is a diterpenoid triepoxide derived from the herb *Tripterygium wilfordii* [8]. As a natural medicine in China for hundreds of years, TPL has been established to possess a broad bioactive spectrum of anti-fertility, immunosuppression, anti-inflammation, anti-cystogenesis, and anti-tumor activities [9]. Mounting evidence suggests that TPL confers anti-cancer activities by suppressing the proliferation and enhancing the apoptosis of different cancer cells, including oral cancer [10-17]. Previously, TPL inhibited proliferation of several cancer cells in vitro and hampered tumor growth and metastases of melanoma, breast cancer, bladder cancer, and gastric carcinoma in mouse models [16]. Chen et al. [17] demonstrated that TPL induces

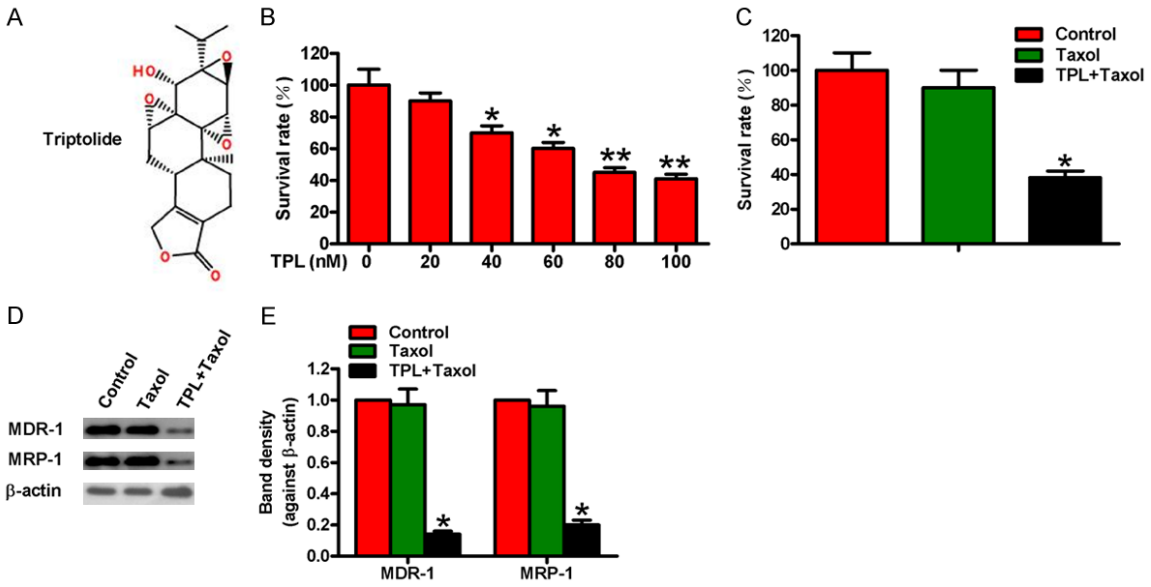

Figure 1. TPL overcame MDR of SAS/Taxol cells. (A) The structure of TPL. (B) SAS/Taxol cells were treated with various concentrations (0, 20, 40, 60, 80, and 100 nM) of TPL for 48 h. CCK-8 assay was conducted to evaluate cell viability. (C-E) SAS/Taxol cells were treated with vehicle control, 80 nM TPL, or 80 nM TPL and 200 ng/ml of Taxol simultaneously. (C) Cell viability was measured by CCK-8 assay. (D) Representative western blot results of MDR1 and MRP1. β-actin was used as the normal control. (E) Quantification of the band density in (D). Data are presented as the mean ± SD of three replicates. $*P < 0.05$, $**P < 0.01$ compared with control group.

prominent growth inhibition and apoptosis in two oral cancer cell lines in vitro and inhibits the tumor growth via apoptosis induction in vivo. In the literature, TPL has been regarded as an adjuvant therapeutic agent that circumvents resistance to current anticancer therapies and enhances the anticancer effectiveness [18]. TPL can overcome MDR in prostate cancer cells by the downregulation of MDR1 expression [19]. In addition, TPL exerts pro-apoptotic and cell cycle arrest activity on drug-resistant human lung cancer A549/Taxol cells [20]. Also, TPL circumvents drug-resistant effects of 5-fluorouracil on KB cells [21]. Furthermore, TPL synergistically enhances the anti-tumor effects of ionizing radiation in oral cancer in vitro and in vivo [22]. However, the effects of TPL on MDR OSCC cells and its potential to overcome MDR have not been explored. Thus, identifying the underlying mechanisms by which TPL suppresses MDR of OSCC will shed light on its precision treatment.

In this study, we investigated the anti-cancer effects of TPL on the Taxol-resistant cell line SAS/Taxol. Therapeutic effects of TPL have also been explored in a xenograft tumor bearing mouse model. It revealed that TPL exerts anti-tumor effects by growth inhibition and apoptosis induction. Intrinsic and extrinsic apoptotic pathway-dependent caspase activation is essential for TPL-induced cell apoptosis. Overall, TPL may be useful for the prevention and treatment for OSCC patients with Taxol resistance.

Materials and methods

Cell culture

The human oral cancer cell line SAS was purchased from Nanjing KeyGen Biotechnology Co. Ltd. (China). SAS cells resistant to Taxol were established as follows. Briefly, SAS cells in the exponential phase of growth were exposed to 200 ng/ml of Taxol (Sigma-Aldrich, St Louis, MO, USA) for 1 month. After 3 months of Taxol initiated treatment, the Taxol-resistant cell line SAS/Taxol was established and then maintained in a drug-free medium and subcultured at least 3 times. SAS and SAS/Taxol cells were cultured in RPMI-1640 medium (Gibco BRL, Gaithersburg, MD, USA) supplemented with 10% bovine calf serum (Gibco), 100 U/ml penicillin, and 100 μg/ml streptomycin (both from Sigma) at 37°C in a humidified atmosphere of 5% CO_2.

Cell viability assay

Cell viability was detected using Cell Counting Kit-8 (CCK-8; Solarbio, Beijing, China) assay. 100 μl SAS and SAS/Taxol cells were seeded onto a 96-well plate at a density of 1×10^4 cells/well. Following overnight incubation, the culture medium was aspirated, and the cells were administered with various doses of TPL (Sigma; the final concentrations were 20, 40, 60, 80 and 100 nM). In addition, the cells were exposed to vehicle control, 200 ng/ml of Taxol, or 200 ng/ml of Taxol + 80 nM of TPL. The cells were then cultivated for 48 h and 10 μl of CCK-8 solutions were added to each well. After incubation for 2 h, the absorbance at 450 nm was measured on a microplate reader (Spectra MAX190, Molecular Devices LLC, Sunnyvale, CA, USA). The results were expressed as a percentage of the control cells.

5-ethyl-2'-deoxyuridine (EdU) incorporation assay

Cell proliferation was assessed using EdU staining (RiboBio, Guangzhou, China) assay. SAS/Taxol cells were seeded onto a 24-well plate at a density of 1×10^5 cells/well. After treatment with or without 80 nM TPL for 48 h, cells were incubated with culture medium containing 20 μM EdU for 2 h, and then fixed with 4% paraformaldehyde (Sigma) for 20 min at room temperature. According to the manufacturer's instructions, cells were incubated with Apollo solution for 30 min and stained with Hoechst 33342 for 15 min. The stained cells were washed with PBS twice before observation. Five random fields were selected from each well and photographed under an inverted fluorescent microscope (Carl-Zeiss, Berlin, Germany).

Colony formation assay

A total of 1×10^3 SAS/Taxol cells were grown in 6-well plates pre-coated with 1% agar (Sigma). After treatment with or without 80 nM TPL for 48 h, fresh culture medium was replaced and the cells were cultured for another 12 d. The cells were fixed with methanol and the colonies were stained with 0.4% crystal violet (Sigma) and counted under a microscope (Olympus, Tokyo, Japan). Five random fields in each well were chosen to calculate the total number of colonies.

Cell cycle analysis

SAS/Taxol cells (3×10^5 cells/well) were seeded onto six-well plates. Following overnight incubation, cells were treated with or without 80 nM TPL for 48 h, and then were harvested and centrifuged. For the cell cycle distribution analysis, the supernatant was discarded, and attached cells were harvested and fixed in cold 70% ethanol overnight at -20°C. Cell cycle distribution was analyzed by using a BD FACS Calibur flow cytometer (BD Bioscience, San Jose, CA, USA) according to the manufacturer's instructions for the propidium iodide (PI; Sigma) staining kit.

Apoptosis analysis by flow cytometry

Cell apoptosis was evaluated by flow cytometry. 3×10^5 SAS/Taxol cells were seeded onto six-well plates. After reaching 80% confluence, cells were treated with or without 80 nM TPL for 48 h, and then were harvested, centrifuged, and resuspended in binding buffer. As per the manufacturer's protocol, 10 μl of ready-to-use Annexin V-fluorescein isothiocyanate (FITC; BD Bioscience) was added into the mixture, incubated at 37°C for 15 min, and counterstained with 5 μl PI in the dark for 30 min. Annexin V-FITC and PI fluorescence were assessed using BD FACS Calibur flow cytometer (BD Bioscience), and the data were analyzed by CellQuest software (BD Bioscience).

Measurement of mitochondrial permeability potential (MMP)

MMP loss was measured using JC-1 assay [23]. In brief, at 48 h after treatment with or without TPL, SAS/Taxol cells were stained with the cationic dye JC-1 (MitoPT, Immunohistochemistry Technologies, Bloomington, MN), which exhibits potential-dependent accumulation in mitochondria. At low membrane potential, JC-1 exists as a monomer and produces a green fluorescence (emission at 527 nm). At high membrane potential, JC-1 forms J aggregates (emission at 590 nm) and produces a red fluorescence.

Measurement of caspase-3, -8, and -9 activities

Caspase-3 activity was determined using the Caspase-3/CPP32 Colorimetric Assay Kit (Bio-

Vision, Palo Alto, CA, USA), and caspase-8, -9 activity was tested using caspase-8 and caspase-9 Fluorimetric Assay (R&D Systems, Minneapolis, MN, USA). Briefly, 3×10^5 SAS/Taxol cells were seeded onto six-well plates. After reaching 80% confluence, cells were treated without or with 80 nM TPL for 48 h. Cells were harvested, lysed, and centrifuged, and then the supernatant was collected. Caspase-3, -8, and -9 activities were measured by analyzing the cleavage of the colorimetric or fluorometric substrates.

Western blot analysis

At 48 h after treatment with or without 80 nM TPL or after exposure to vehicle control, 200 ng/ml of Taxol, or 200 ng/ml of Taxol + 80 nM of TPL, SAS/Taxol cells were lysed and total protein was collected and measured by BCA protein assay kit (Beyotime, Haimen, China). Proteins were separated by 10% sodium dodecyl sulfate-polyacrylamide gel electrophoresis and transferred onto polyvinylidene fluoride membranes (Millipore, Hong Kong, China). After blocking with 5% nonfat milk diluted in Tris-buffered saline buffer containing 0.1% Tween-20 (pH 7.4) for 2 h at room temperature, the membranes were incubated with primary antibodies against MDR1, MRP1 (both from Cell Signaling Technology, Danvers, Massachusetts, USA), Cyclin D1, Bax, Bcl-2, cytochrome C (Cyt C), apoptosis inducing factor (AIF), Bid, caspase-8, caspase-9, caspase-3, cleaved (cl)-caspase-3, and β-actin (all from Abnova, Taiwan, China) at 4°C overnight. After 1 h of incubation with the appropriate horseradish peroxidase-conjugated secondary antibodies, the bands were detected with an enhanced chemiluminescence kit (Amersham Pharmacia Biotech, Buckinghamshire, UK). Protein band density was quantified using Quantity One software (Bio-Rad, Berkeley, CA, USA).

Terminal deoxynucleotidyl transferase-mediated dUTP nick end labeling (TUNEL) assay

Apoptosis *in situ* was evaluated by TUNEL assay following the manufacturer's protocol (Roche, Mannheim, BW, Germany). For cells, at 48 h after treatment with or without TPL, SAS/Taxol cells were fixed with 80% glycerol at room temperature. Cells were washed with PBS twice and permeabilized with 2% Triton X-100. The FITC-labeled terminal deoxynucleotidyl transferase (TdT) nucleotide mix (Promega, Madison, WI, USA) was added into each well and incubated at 37°C for 1 h and then counterstained with 10 mg/ml 4',6-diamidino-2-phenylindole (Sigma) for 30 min. For tissues, tumor samples removed from the mice were formalin fixed and paraffin-embedded. 4 μm thickness sections were stained and examined. TUNEL-positive cells were imaged and counted by fluorescence microscopy (Carl-Zeiss).

Xenograft tumor model

Ten SCID mice (6-week-old) were purchased from Institute of Zoology, Chinese Academy of Sciences (Beijing, China) and maintained under specific pathogen-free conditions with sterile food and chlorinated sterile water. The experiments were carried out in strict accordance with the recommendations in the Guide for the Care and Use of Laboratory Animals of the Chinese PLA General Hospital (Beijing, China). The protocol was approved by the Committee on the Ethics of Animal Experiments of Chinese PLA General Hospital.

For xenograft tumor model establishment, all the mice were subcutaneously injected with 2×10^6 SAS/Taxol cells into the hind legs. After 3 days, the mice were randomly divided into 2 groups (n = 5 per group). In one group, the mice were administered with TPL (0.15 mg/kg/day) via intraperitoneal injections and continuously administrated for 4 weeks. The mice in the other group were intraperitoneally injected with vehicle (PBS). The tumor size was measured by the calipers once a week and the tumor volume was calculated using the formula $V = 1/2 \times (\text{length} \times \text{width}^2)$. At the end of treatment, the mice were sacrificed, and the tumors were removed, weighed, and photographed. Tumor tissues were fixed, embedded, and sectioned for TUNEL assay.

Statistical analysis

Data are expressed as the mean ± standard derivation (SD). The statistical differences were determined by Student's two-tailed t-test for two groups and one-way analysis of variance among multiple groups. SPSS version 16.0 software (SPSS Inc., Chicago, IL, USA) was applied for statistical analyses. $P < 0.05$ was considered statistically significant.

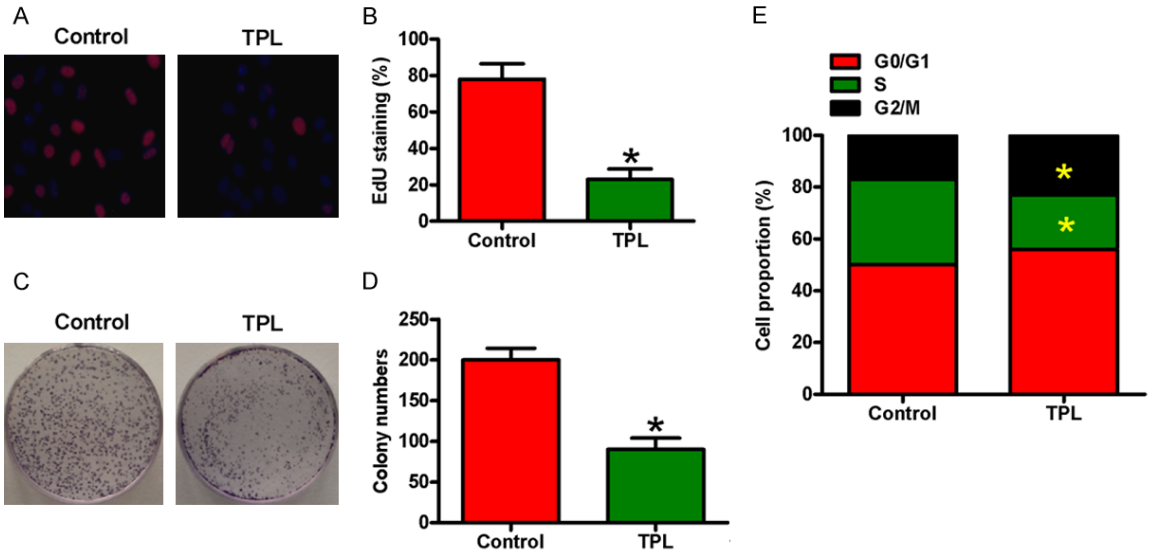

Figure 2. TPL hindered SAS/Taxol cell proliferation. SAS/Taxol cells were treated with 80 nM TPL for 48 h. A. EdU incorporation assay was performed to examine cell proliferation. B. The quantification of EdU-staining cells. C. Colony formation assay was carried out to determine cell proliferation. D. Colony formation number was calculated 12 days later. E. Flow cytometry was conducted to show the cell cycle distribution. Proportion of the cells in different phases was calculated. Data are presented as the mean ± SD of three replicates. *$P < 0.05$ compared with control group.

Results

TPL overcomes Taxol resistance of SAS/Taxol cells

To investigate the effects of TPL on SAS/Taxol cell proliferation, we treated SAS/Taxol cells with various concentrations (0, 20, 40, 60, 80, and 100 nM) of TPL for 48 h. As shown in **Figure 1B**, CCK-8 assay showed that TPL reduced the viability of SAS/Taxol cells in a dose-dependent manner. Moreover, we found that treatment with 80 nM or 100 nM TPL exhibited more growth inhibition than other doses and time points, and no significance existed in both groups. Thus, treatment with 80 nM TPL was selected for subsequent experiments.

To address the effects of TPL on MDR, we treated SAS/Taxol cells with 80 nM TPL and 200 ng/ml of Taxol simultaneously. Cell viability results demonstrated that TPL increased the sensitivity of SAS/Taxol cells to Taxol-induced cell proliferation inhibition (**Figure 1C**). We also examined the influence of TPL on the expression of MDR-associated proteins (MDR1 and MRP1) by western blot. As shown in **Figure 1D** and **1E**, the expression of MDR1 and MRP1 was much lower in SAS/Taxol cells with TPL and Taxol co-treatment than that in the control- or Taxol alone-treated cells. Taken together, these results suggest that TPL overcomes Taxol resistance in oral cancer cells by inhibiting the expression of MDR1 and MRP1.

TPL represses the proliferation of SAS/Taxol cells

We next explore the functions of TPL on the proliferation of SAS/Taxol cells. EdU assay revealed that TPL significantly inhibited the proliferation of SAS/Taxol cells compared with the control cells (**Figure 2A** and **2B**). Consistently, the suppressive effect of TPL on SAS/Taxol cell proliferation was confirmed by colony formation assay (**Figure 2C** and **2D**). We further examined the cell cycle phase distribution of SAS/Taxol cells after TPL treatment. Flow cytometry analysis showed that TPL induced considerable S phase accumulation and G0/G1 phase reduction in SAS/Taxol cells (**Figure 2E**). Collectively, these data indicate that TPL inhibits SAS/Taxol cell proliferation by inducing S phase arrest.

TPL promotes SAS/Taxol cell apoptosis

Subsequently, we examined whether TPL induced apoptosis of SAS/Taxol cells. Flow cytometry results showed a significant increase in apoptotic SAS/Taxol cells with TPL treatment

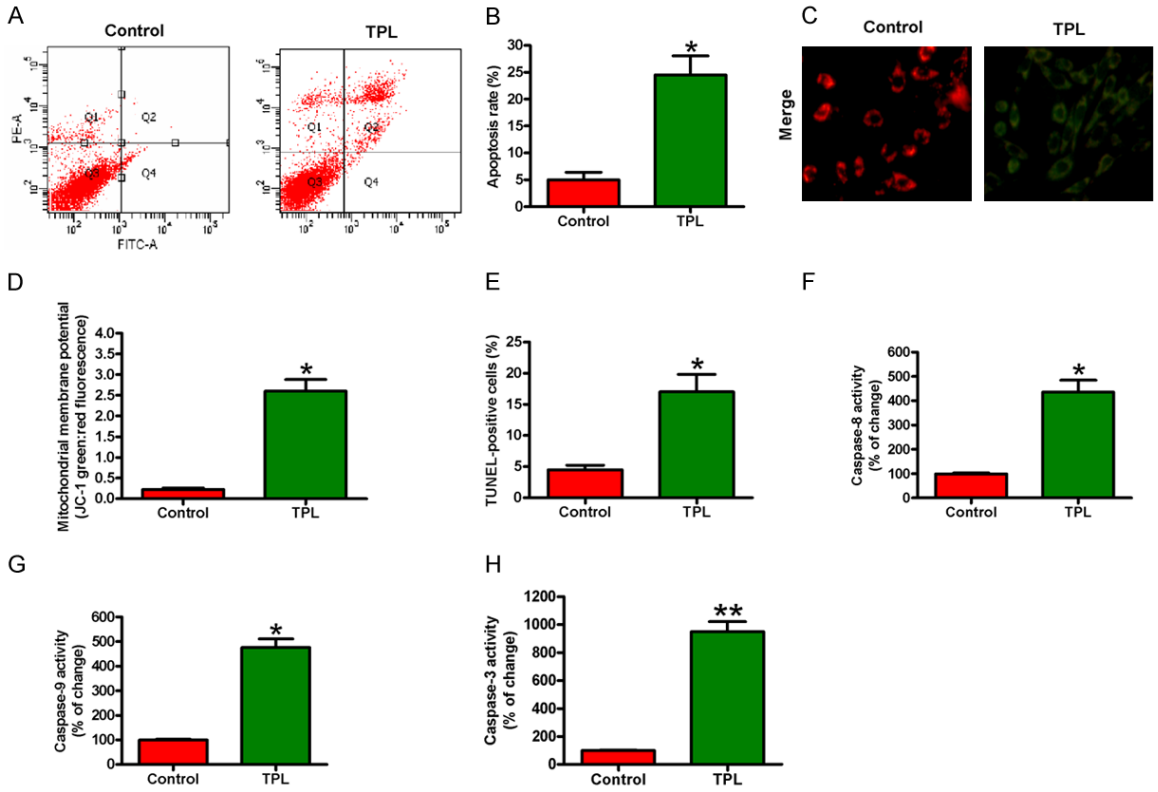

Figure 3. TPL caused SAS/Taxol cell apoptosis. SAS/Taxol cells were treated with 80 nM TPL for 48 h. (A) Annexin V-FITC/PI staining was analyzed to assess SAS/Taxol cell apoptosis. (B) The quantification of apoptotic cells. (C) Representative images of JC-1 staining. (D) Quantification of MMP. (E) TUNEL assay was performed and the percentage of TUNEL-positive cells was calculated. (F-H) The activities of caspase-8 (F), caspase-9 (G), and caspase-3 (H) were measured. Data are presented as the mean ± SD of three replicates. $*P < 0.05$, $**P < 0.01$ compared with control group.

(**Figure 3A** and **3B**). JC-1 assay demonstrated that TPL facilitated mitochondrial membrane potential loss of SAS/Taxol cells (**Figure 3C** and **3D**). TUNEL also revealed that TPL caused a large number of apoptotic SAS/Taxol cells as shown by the TUNEL-positive cells (**Figure 3E**). Apoptosis is mediated by the activation of caspase cascades [24]. We therefore addressed whether TPL induced apoptosis by caspase signaling in SAS/Taxol cells. After treatment with 80 nM TPL for 48 h, caspase-3, -8 and -9 activities in SAS/Taxol cells were examined. As depicted in **Figure 3F-H**, TPL resulted in considerable enhancement of caspase-3, -8 and -9 activities. These results revealed that TPL caused SAS/Taxol cell apoptosis partly by activating a series of caspases.

TPL-induced SAS/Taxol cell apoptosis through the intrinsic and extrinsic apoptotic pathways

To probe the molecular mechanism by which TPL induces the cell cycle arrest and apoptosis of SAS/Taxol cells, western blot assay was performed to evaluate the expression of some cell cycle- and apoptosis-associated proteins. As shown in **Figure 4A** and **4B**, TPL remarkably decreased the protein level of Cyclin D1. For apoptosis- associated proteins, TLP induced significant upregulation in the expression of Bax, Bid, Cyt C, AIF, caspase-8 caspase-9, and cl-caspase-3 in SAS/Taxol cells; however, TLP markedly decreased Bcl-2 level (**Figure 4A** and **4B**). These data demonstrated that TPL triggered SAS/Taxol cell apoptosis by activating caspase cascades.

TPL hinders tumor growth of SAS/Taxol cells in vivo

To determine whether the anti-tumor effects of TPL on SAS/Taxol cells in vivo, a xenograft tumor-bearing model was established by using the SCID mice subcutaneously injected with 2×10^6 SAS/Taxol cells. As depicted in **Figure 5A**, TPL administration significantly reduced

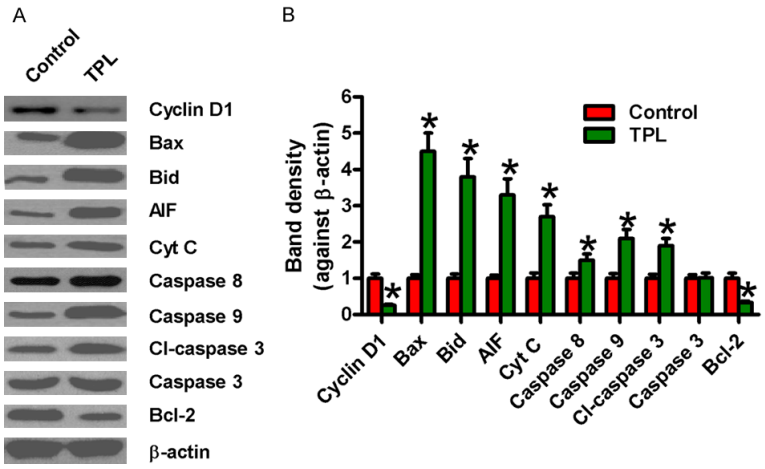

Figure 4. TPL regulated apoptosis-associated protein expression in SAS/Taxol cells. SAS/Taxol cells were treated with 80 nM TPL for 48 h. (A) Representative western blot results of Cyclin D1, Bcl-2, Bax, Bid, Cyt C, AIF, caspase-8, caspase-9, caspase-3, and cl-caspase-3. β-actin was used as the endogenous control. (B) Band density of western blots in (A). Data are presented as the mean ± SD of three replicates. *$P < 0.05$ compared with control group.

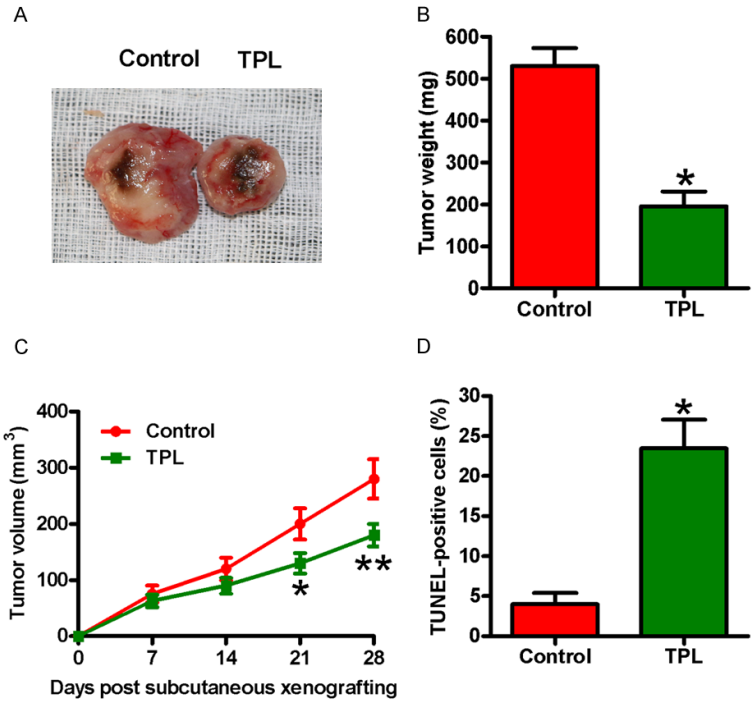

Figure 5. TPL induced the growth inhibition and apoptosis of primary tumors in mice. SCID mice were subcutaneously injected with 2 × 10^6 SAS/Taxol cells into the hind legs. Beginning 3 days later, the mice were divided into two groups, one of which was given daily intraperitoneal injections of TPL (0.15 mg/kg/day), whereas the other was given vehicle controls. At the end of 4 weeks, the mice were sacrificed, and the tumors were removed, photographed, and weighed. (A) Representative images of tumors and (B) quantification of tumor weights. (C) Tumor volume of the subcutaneous xenograft model was measured once a week after SAS/Taxol cell implantation for 4 weeks. (D) The apoptosis of tumor tissues was evaluated by TUNEL assay. Data are presented as the mean ± SD of three replicates. *$P < 0.05$, **$P < 0.01$ compared with control group.

tumor growth. The tumor weight was significantly reduced in the TPL-treated mice compared with tumor-bearing control mice (**Figure 5B**). The tumor volume of mice treated with TPL was markedly smaller than those treated with vehicle (**Figure 5C**). In addition, TPL resulted in much higher apoptotic cells of the tumor tissues (**Figure 5D**). Overall, the data demonstrate that TPL has a strong inhibitory effect on tumor growth in vivo.

Discussion

In this study, TPL exerted inhibitory effects on drug-resistant human oral cancer SAS/Taxol cells. Key findings were as follows. First, TPL circumvented Taxol resistance of SAS/Taxol cells. Second, TPL reduced SAS/Taxol cell proliferation. Third, TPL triggered apoptosis of SAS/Taxol cells. Fourth, TPL increased activities and induced activation of caspase-3, -8 and -9 in SAS/Taxol cells. Fifth, TPL enhanced the expression of pro-apoptotic protein (AIF, Bax and Bid) and Cyt C release while decreased the level of Cyclin D1 and Bcl-2 in SAS/Taxol cells. Last, TPL hampered tumor formation of SAS/Taxol cells in vivo. Together, TPL conferred suppressive effects on drug-resistant human oral cancer SAS/Taxol cells.

Chemotherapy is a widely used and an effective strategy for cancer therapy [25]. However, the cytostatic and cytotoxic effects of chemotherapy to induce apoptosis in OSCC might be restricted due to an inducible cellular mechanism called MDR [5]. In particular, the transporter MDR1 encoded by the *MDR1* gene is one of

the most important mechanisms that contribute to MDR [6]. Several investigations revealed the role of TPL in regulating the efflux transporters to reverse MDR [19-21, 26]. Guo et al. [19] reported that TPL overcomes MDR in adriamycin-resistent prostate cancer cells via downregulation of MDR1 expression, and Li et al. [26] proved that TPL reverses the adriamycin resistance in K562/A02 cells via downregulation of MDR1 expression. Another study indicated that TPL displays strong anti-cancer effects on KB-7D cells with MRP overexpression and KB-tax cells overexpressing MDR by downregulating MRP and MDR expressions. TPL combined with 5-fluorouracil shows synergistic anti-tumor activities against cancer resistant xenografts in vivo [21]. Furthermore, TPL enhances anti-tumor activity of irradiation for the treatment of oral cancer [22]. In this study, we demonstrated that TPL enhanced Taxol sensitivity of SAS/Taxol cells by downregulation of MRP1 and MDR1 levels.

Preclinical studies indicated that TPL inhibits cell proliferation, induces cell apoptosis, inhibits tumor metastasis and enhances the effect of other therapeutic methods in various cancer cell lines [10, 11]. Reportedly, TPL inhibited the proliferation and induced the apoptosis in liver cancer HepG2 cells [16] and various leukemic cell lines and primary acute myeloid leukemia blasts [27]. Intriguingly, TPL reduced the viability, motility, and angiogenesis in SAS oral cancer cells [28]. Hou et al. [18] reported that TPL attenuates MDR of cancer cells and enhances sensitization of chemo-therapeutic drugs for cancer therapy through proliferation inhibition and apoptosis induction. For example, TPL induces the apoptosis of cisplatin-resistant nasopharyngeal cancer cell line HNE1/DDP by increasing expression of Bax and caspase-9, and reducing Bcl-2 and Mcl-1 levels and synergizes the toxicities of cisplatin [29]. TPL synergistically enhances the anti-tumor effects of cisplatin in cisplatin resistant human bladder cancer cells [30]. Also, combination treatment with TPL and cisplatin induces cell cycle arrest via Cyclin D1 and Cyclin E1 expression and promotes apoptosis accompanied by increased expression of caspase-3, -8, and -9, and Cyt C [30]. In the literature, TPL notably induces proliferation inhibition, cell cycle arrest, and apoptosis of A549/Taxol cells [20]. Consistently, we found that TPL hampered the proliferation and cell cycle progression and promoted the apoptosis of oral cancer SAS/Taxol cells in vitro. TPL also hindered tumor growth and induced cell apoptosis in vivo.

A defect in apoptosis is a common phenomenon in many types of cancer resistance to therapy [31]. Generally, apoptosis is mediated by caspase activation, an event that is tightly regulated and involves two major pathways, including the intrinsic and extrinsic pathways [32]. The extrinsic pathway is initiated by the binding of death receptors with their death initiating ligands and subsequently leads to the activation of caspase-8. Activated caspase-8 can either directly cleave or activate caspase-7 or caspase-3, thereby promoting apoptosis. The intrinsic pathway is modulated by the activation of BH3-only proteins sensing different types of cell stress and then activating Bax/Bak at the mitochondrial outer membrane which leads to release of different apoptosis-mediating molecules, such as Cyt C and subsequently activates caspase-9. Caspase-9 can cleave and result in caspase-3 and caspase-7 activation, thus triggering apoptotic cell death [32]. In both pathways, several anti-apoptotic proteins and pro-apoptotic signals are involved, such as Bcl-2 family proteins, which are attractive targets for anticancer resistance [33]. Reportedly, Bcl-2 family affords an essential role in regulating the apoptotic pathway [34]. Bax is a pro-apoptotic protein, while Bcl-2 possesses anti-apoptotic properties by stabilizing mitochondrial membrane and suppressing the release of Cyt C [35]. Carter et al. [27] reported that TPL induces caspase-dependent cell death mediated via the mitochondrial pathway in leukemic cells. Furthermore, TPL significantly elevates caspase-3, -8, and -9 activities in two oral cancer cells [17]. Consistent with these findings, we here observed significant enhancement of caspase-3, -8, and -9 activities as well as upregulation of Bax, AIF, Cyt C, caspase-3, -8 and -9, and downregulation of Cyclin D1 and Bcl-2 in TPL-treated SAS/Taxol cells, indicating that TPL triggered SAS/Taxol cell apoptosis depending on both the intrinsic and extrinsic apoptotic pathways.

In this study, we found that TPL exerted anticancer effects on SAS/Taxol cells by enhancing cytotoxicity, repressing proliferation, and inducing apoptosis. The apoptosis induction of TPL

was partly relying on intrinsic and extrinsic apoptotic pathways-mediated caspase activation. Thus, TPL is a potential chemotherapy and chemoprevention agent of Taxol-resistant oral cancer.

Acknowledgements

This study was supported by grants from the National Nature Science Foundation of China (No. 81870824 and No. 81501885) and China Postdoctoral Science Foundation (No. 45424).

Disclosure of conflict of interest

None.

Address correspondence to: Dr. Ning Wen, Institute of Stomatology, Chinese PLA General Hospital, No. 28 Fuxing Road, Haidian District, Beijing, China. Tel: +86-10-68182255; Fax: +86-10-68182255; E-mail: ningwenvip@126.com

References

[1] Torre LA, Bray F, Siegel RL, Ferlay J, Lortet-Tieulent J and Jemal A. Global cancer statistics, 2012. CA Cancer J Clin 2015; 65: 87-108.

[2] Huang SH and O'Sullivan B. Oral cancer: current role of radiotherapy and chemotherapy. Med Oral Patol Oral Cir Bucal 2013; 18: e233-240.

[3] Bonner JA, Harari PM, Giralt J, Azarnia N, Shin DM, Cohen RB, Jones CU, Sur R, Raben D, Jassem J, Ove R, Kies MS, Baselga J, Youssoufian H, Amellal N, Rowinsky EK and Ang KK. Radiotherapy plus cetuximab for squamous-cell carcinoma of the head and neck. N Engl J Med 2006; 354: 567-578.

[4] Gottesman MM. Mechanisms of cancer drug resistance. Annu Rev Med 2002; 53: 615-627.

[5] Richard V, Sebastian P, Nair MG, Nair SN, Malieckal TT, Santhosh Kumar TR and Pillai MR. Multiple drug resistant, tumorigenic stem-like cells in oral cancer. Cancer Lett 2013; 338: 300-316.

[6] Wu CP, Hsieh CH and Wu YS. The emergence of drug transporter-mediated multidrug resistance to cancer chemotherapy. Mol Pharm 2011; 8: 1996-2011.

[7] Sinha N, Mukhopadhyay S, Das DN, Panda PK and Bhutia SK. Relevance of cancer initiating/stem cells in carcinogenesis and therapy resistance in oral cancer. Oral Oncol 2013; 49: 854-862.

[8] Chen X, Murakami T, Oppenheim JJ and Howard OM. Triptolide, a constituent of immunosuppressive Chinese herbal medicine, is a potent suppressor of dendritic-cell maturation and trafficking. Blood 2005; 106: 2409-2416.

[9] Zhou ZL, Yang YX, Ding J, Li YC and Miao ZH. Triptolide: structural modifications, structure-activity relationships, bioactivities, clinical development and mechanisms. Nat Prod Rep 2012; 29: 457-475.

[10] Meng C, Zhu H, Song H, Wang Z, Huang G, Li D, Ma Z, Ma J, Qin Q, Sun X and Ma J. Targets and molecular mechanisms of triptolide in cancer therapy. Chin J Cancer Res 2014; 26: 622-626.

[11] Yang S, Chen J, Guo Z, Xu XM, Wang L, Pei XF, Yang J, Underhill CB and Zhang L. Triptolide inhibits the growth and metastasis of solid tumors. Mol Cancer Ther 2003; 2: 65-72.

[12] Zhou H, Liu Y, Wang C, Liu L, Wang H, Zhang Y, Long C and Sun X. Triptolide inhibits Epstein-Barr nuclear antigen 1 expression by increasing sensitivity of mitochondria apoptosis of nasopharyngeal carcinoma cells. J Exp Clin Cancer Res 2018; 37: 192.

[13] Jiang J, Song X, Yang J, Lei K, Ni Y, Zhou F and Sun L. Triptolide inhibits proliferation and migration of human neuroblastoma SH-SY5Y cells by upregulating microRNA-181a. Oncol Res 2018; 26: 1235-1243.

[14] Kong J, Wang L, Ren L, Yan Y, Cheng Y, Huang Z and Shen F. Triptolide induces mitochondria-mediated apoptosis of Burkitt's lymphoma cell via deacetylation of GSK-3beta by increased SIRT3 expression. Toxicol Appl Pharmacol 2018; 342: 1-13.

[15] Song JM, Molla K, Anandharaj A, Cornax I, MG OS, Kirtane AR, Panyam J and Kassie F. Triptolide suppresses the in vitro and in vivo growth of lung cancer cells by targeting hyaluronan-CD44/RHAMM signaling. Oncotarget 2017; 8: 26927-26940.

[16] Sun YY, Xiao L, Wang D, Ji YC, Yang YP, Ma R and Chen XH. Triptolide inhibits viability and induces apoptosis in liver cancer cells through activation of the tumor suppressor gene p53. Int J Oncol 2017; 50: 847-852.

[17] Chen YW, Lin GJ, Chia WT, Lin CK, Chuang YP and Sytwu HK. Triptolide exerts anti-tumor effect on oral cancer and KB cells in vitro and in vivo. Oral Oncol 2009; 45: 562-568.

[18] Hou ZY, Tong XP, Peng YB, Zhang BK and Yan M. Broad targeting of triptolide to resistance and sensitization for cancer therapy. Biomed Pharmacother 2018; 104: 771-780.

[19] Guo Q, Nan XX, Yang JR, Yi L, Liang BL, Wei YB, Zhu N, Hu SB, Zhang H, Luo Y and Xu YF. Triptolide inhibits the multidrug resistance in prostate cancer cells via the downregulation of MDR1 expression. Neoplasma 2013; 60: 598-604.

[20] Xie CQ, Zhou P, Zuo J, Li X, Chen Y and Chen JW. Triptolide exerts pro-apoptotic and cell cycle arrest activity on drug-resistant human lung cancer A549/Taxol cells via modulation of MAPK and PI3K/Akt signaling pathways. Oncol Lett 2016; 12: 3586-3590.
[21] Chen YW, Lin GJ, Chuang YP, Chia WT, Hueng DY, Lin CK, Nieh S and Sytwu HK. Triptolide circumvents drug-resistant effect and enhances 5-fluorouracil antitumor effect on KB cells. Anticancer Drugs 2010; 21: 502-513.
[22] Chen YW, Lin GJ, Hueng DY, Huang SH, Chia WT, Shieh YS, Ma KH and Sytwu HK. Enhanced anti-tumor activity of triptolide in combination with irradiation for the treatment of oral cancer. Planta Med 2014; 80: 255-261.
[23] Li S, Lv X, Zhai K, Xu R, Zhang Y, Zhao S, Qin X, Yin L and Lou J. MicroRNA-7 inhibits neuronal apoptosis in a cellular Parkinson's disease model by targeting Bax and Sirt2. Am J Transl Res 2016; 8: 993-1004.
[24] Nicholson DW and Thornberry NA. Caspases: killer proteases. Trends Biochem Sci 1997; 22: 299-306.
[25] Longley DB, Harkin DP and Johnston PG. 5-fluorouracil: mechanisms of action and clinical strategies. Nat Rev Cancer 2003; 3: 330-338.
[26] Li H, Hui L, Xu W, Shen H, Chen Q, Long L and Zhu X. Modulation of P-glycoprotein expression by triptolide in adriamycin-resistant K562/A02 cells. Oncol Lett 2012; 3: 485-489.
[27] Carter BZ, Mak DH, Schober WD, McQueen T, Harris D, Estrov Z, Evans RL and Andreeff M. Triptolide induces caspase-dependent cell death mediated via the mitochondrial pathway in leukemic cells. Blood 2006; 108: 630-637.
[28] Yang CY, Lin CK, Lin GJ, Hsieh CC, Huang SH, Ma KH, Shieh YS, Sytwu HK and Chen YW. Triptolide represses oral cancer cell proliferation, invasion, migration, and angiogenesis in co-inoculation with U937 cells. Clin Oral Investig 2017; 21: 419-427.
[29] Wang X, Zhang JJ, Sun YM, Zhang J, Wang LR, Li JC and Liu H. Triptolide induces apoptosis and synergizes with cisplatin in cisplatin-Resistant HNE1/DDP nasopharyngeal cancer cells. Folia Biol (Praha) 2015; 61: 195-202.
[30] Ho JN, Byun SS, Lee S, Oh JJ, Hong SK, Lee SE and Yeon JS. Synergistic antitumor effect of triptolide and cisplatin in cisplatin resistant human bladder cancer cells. J Urol 2015; 193: 1016-1022.
[31] Baguley BC. Multidrug resistance in cancer. Methods Mol Biol 2010; 596: 1-14.
[32] Mohammad RM, Muqbil I, Lowe L, Yedjou C, Hsu HY, Lin LT, Siegelin MD, Fimognari C, Kumar NB, Dou QP, Yang H, Samadi AK, Russo GL, Spagnuolo C, Ray SK, Chakrabarti M, Morre JD, Coley HM, Honoki K, Fujii H, Georgakilas AG, Amedei A, Niccolai E, Amin A, Ashraf SS, Helferich WG, Yang X, Boosani CS, Guha G, Bhakta D, Ciriolo MR, Aquilano K, Chen S, Mohammed SI, Keith WN, Bilsland A, Halicka D, Nowsheen S and Azmi AS. Broad targeting of resistance to apoptosis in cancer. Semin Cancer Biol 2015; 35 Suppl: S78-S103.
[33] Morin PJ. Drug resistance and the microenvironment: nature and nurture. Drug Resist Updat 2003; 6: 169-172.
[34] Adams JM and Cory S. The Bcl-2 protein family: arbiters of cell survival. Science 1998; 281: 1322-1326.
[35] Kuida K, Haydar TF, Kuan CY, Gu Y, Taya C, Karasuyama H, Su MS, Rakic P and Flavell RA. Reduced apoptosis and cytochrome c-mediated caspase activation in mice lacking caspase 9. Cell 1998; 94: 325-337.